MDPI

Article

Water desalination using polyelectrolyte hydrogel: Gibbs ensemble modeling

Mikhail Laktionov [1,2], Lucie Nová [1] and Oleg V. Rud [1,3]*

[1] Department of Physical and Macromolecular Chemistry, Faculty of Science, Charles University in Prague, Czech Republic; e-mail@e-mail.com
[2] St. Petersburg National Research University of Information Technologies, Mechanics and Optics, St. Petersburg, Russia; e-mail@e-mail.com
[3] Institute of Macromolecular Compounds of Russian Academy of Sciences, Saint-Petersburg, Russia; e-mail@e-mail.com
* Correspondence: oleg.rud@natur.cuni.cz;

Abstract: Polyelectrolyte hydrogels can absorb a big amount of water across an osmotic membrane as a result of their swelling pressure. On the other hand, the insoluble cross-linked hydrogel network enables dewatering under the influence of external (thermal and/or mechanical) stimuli. Moreover, from a thermodynamic perspective, the polyelectrolyte hydrogel is already an osmotic membrane. These above-mentioned properties designate hydrogels as excellent candidates for use in desalination, allowing, at the same time, to avoid the use of expensive membranes. In this article, we present our recent theoretical study of polyelectrolyte hydrogel usage for water desalination. Employing a coarse-grained model and the Gibbs ensemble, we modeled the thermodynamic equilibrium between coexisting gel phase and the supernate aqueous salt solution phase. We performed a sequence of step-by-step hydrogel swellings and compressions in *open* and *closed* systems, *i. e.* in equilibrium with a big and with a comparably small reservoir of aqueous solutions. The swelling in *open system* causes the removal of ions from the big reservoir, whereas the compression in *closed system* causes the decrease of the salt concentration in the small reservoir. We modeled this stepwise process of continuous decrease of water salinity from seawater up to freshwater concentrations and estimated the energy costs of the process to be comparable with reverse osmosis.

Keywords: polyelectrolye hydrogel; simulation; desalination

Citation: Lastname, F.; Lastname, F.; Lastname, F. Title. *Journal Not Specified* **2022**, *1*, 0. https://doi.org/

Received:
Accepted:
Published:

1. Introduction

Wastewater treatment and technology are one of the greatest concerns of modern society. The waste water has to be disposed of both biological [1] and chemical [2,3] pollutants. Most importantly, water treatment technologies are needed for the still increasing demand on the production of potable water from the brine, *i.* e. for desalination.

1.1. Water desalination technologies

Two basic approaches for separating water from salt are present in modern desalination technology [4,5].

The first approach is distillation, which uses heat to cause a phase change of the water to vapor. The vapor phase is separated from the brine and condenses to liquid fresh water. The released condensation energy is directed back to ~~heating~~ heat the feed solution. Distillation processes were the first desalination techniques conducted on a large commercial scale and still account for a large portion of the modern world's desalination capacity.

The second approach is to physically separate the brine components using an osmotic membrane transparent only for water molecules, which move in response to ~~a~~ the difference in water chemical potential~~difference~~. In the context of our study, we will mention the

reverse osmosis process (RO) ~~—~~ as the major process of all the modern desalination industry, and the newly emerging membrane technology — forward osmosis (FO) [6]. In RO, the difference in water chemical potential originates from a difference in pressures applied to the feed and to product solutions. In FO, the chemical potential difference is due to an addition to solution from one side of the membrane (draw solution) the so-called draw solutes, which are lowering the water chemical potential in draw solution.

Distillation is easy and cheap technology but it is characterized by relatively high energy costs due to the dissipation of thermal energy. ~~On the contrary~~In turn, RO uses expensive osmotic membranes, which need to be replaced regularly because of scaling and fouling. Moreover, RO requires very high operating pressures, ranging from 20 to 200 bar, to let the water pass through the membrane. But, in terms of energy losses, it works close to the thermodynamic limit. Thus, theoretically, per one ion pair transferred from freshwater to salty water, it consumes only the energy equal to the difference between the chemical potentials of the transfered ions.

The absence of large hydraulic pressure in FO process (unlike in RO) allows to reduce the energy consumption in pumping, reduce membrane scaling and fouling, and therefore significantly increase the lifetime of the membranes. In FO, the draw solutes (agents) are dispersed and/or dissolved in water form homogeneous draw solutions. The correct choice of the draw agents is a task of paramount importance. As an osmotically driven process, the draw solute is expected to significantly reduce the water chemical potential, and consequently generate a high osmotic pressure. On the other hand, the draw solute is expected to be easily separated from water [7].

1.2. Hydrogels for desalination~~.~~

Hydrogels are three-dimensional networks of polymer chains that are crosslinked by either physical or chemical bonds. They ~~are able to~~ can entrap large volumes of water attracted by the high concentration of hydrophilic groups. When a dehydrated or deswollen hydrogel uptakes water, its polymer chains extend, creating ~~a~~ swelling pressure. For example, as reported in [8], weakly crosslinked poly(acrylic acid) (PAA) copolymers with polymer volume fractions between 0.03 and 0.30 exhibit a swelling pressure ranging from 0.20–4.23 MPa. ~~Polyelectrolyte~~ *Polyelectrolyte* hydrogels, which are carrying ionic groups on the comonomer units (like PAA), ~~are able to~~ can reject salt ions from the solution, *i.* e. they absorb a solution of lower salinity than that they are equilibrated with.

An important ~~,~~ advantageous aspect of polymer hydrogels is that they can undergo reversible volume change, *i. e.* ~~solution — gel~~ gel — solution volume phase transitions in response to ~~environmental~~ external stimuli. This aspect causes hydrogels to be labeled as 'smart' ~~hydrogels~~materials. Many physical and chemical stimuli have been applied to induce various responses of such smart hydrogels, in particular, to change them from hydrophilic to hydrophobic, thereby releasing water. The physical stimuli include: temperature, solvent composition, light, mechanical pressure, sound, electric and/or magnetic field, whilst the chemical (or biochemical) stimuli include pH, ionic strength, and specific molecular recognition [9–12].

~~The smart properties of hydrogels were utilized for desalination in a recent study by~~ Li *et al.*[13] ~~, where hydrogels have been considered~~ took advantage of the use of smart hydrogels for desalination purposes as draw agents for FO. ~~In this study authors have shown, that hydrogels,~~ They have demonstrated that the hydrogels are able to absorb water across the FO membrane due to their swelling and osmotic pressure and allow dewatering under the influence of stimuli (thermal and/or mechanical), due to their insoluble cross-linked polymer network. ~~For instance, Li *et al.*~~Li *et al.*have proposed the use of hydrogel ~~made of~~ based on thermoresponsive polyelectrolyte — copolymer of poly-N-isopropyl acrylamide (p-NIPAAm) and polyacrylic acid (p-AA). Depending on the temperature ~~the network of the gel appears to be~~ this gel network is either hydrophilic or hydrophobic~~. In the hydrophilic state, the gel is used as a draw solute accumulating water~~

inside , then in the hydrophobic state, , so it accumulates water inside the water releases out network in its hydrophilic state, but it releases the water out in its hydrophobic state.

Moreover, from From a thermodynamics perspective, the polyelectrolyte hydrogel itself is an osmotic membrane generating Donnan potential, which rejects ions between outer and inner solutions [14]. Such a view on hydrogels was employed in a series of works by the group of prof. Wilhelm (see for example [15,16]). The authors of these works proposed to get rid of the osmotic membrane and simply use only micro filtration microfiltration to compress the hydrogel squeezing out the accumulated inside the gel solution. In their methodfirst, the deswollen hydrogel was first equilibrated with saline water feed. During the equilibration, the gel was swellingabsorbing , absorbing the water. Then it was taken out from the feed solution and mechanically squeezed by means of a microfiltration membrane. The squeezed out brine was obtained squeezed-out brine was found, to have lower salinity than the feed water.

A similar approach was used by Ali *et al.*[17]. In their study Here the authors used the thermosensitive gel was used (based on copolymers p-NIPAAm and p-AA), so and instead of physical compression, the dewatering was done by an external heating stimulus (sunlight). At night the gel was equilibrating The gel was equilibrated with feed water and at during the night, and, in the daytime, under sunlight, the gel was shrinking and releasing the collected inside releasing the solution.

1.3. Physics behind the desalination process.

Since the polyelectrolyte gel has its own charges and its own neutralizing counterions, the density of mobile ions (which are able to can freely enter and leave the gel) in gel inside the gel network appears to be smaller than their density outside the gel. Therefore the internal solution of in the gel has a lower density of mobile ions than that in the solution outside. In that sense, the gel acts as an osmotic membrane separating solutions [18]. The driving force of the separation is the Donnan potentialoriginated , which originates from the charges of in the hydrogel network. The density of mobile ions difference between ions concentrationsdifference between the densities (concentrations) of the mobile ions in the internal and external solutions is defined by Donnan law [19]

$$\frac{c^{\text{gel}}_{\text{Cl}^-}}{c_{\text{s}}} = \frac{c_{\text{s}}}{c^{\text{gel}}_{\text{Na}^+}} = \sqrt{1+\left(\frac{\alpha}{2c_{\text{s}}V_{\text{gel}}}\right)^2} \pm \frac{\alpha}{2c_{\text{s}}V_{\text{gel}}}$$

$$\frac{c^{\text{gel}}_{\text{Cl}^-}}{c_{\text{s}}} = \frac{c_{\text{s}}}{c^{\text{gel}}_{\text{Na}^+}} = \sqrt{1+\left(\frac{\alpha}{2c_{\text{s}}v_{\text{gel}}}\right)^2} \pm \frac{\alpha}{2c_{\text{s}}v_{\text{gel}}} \tag{1}$$

where $c^{\text{gel}}_{\text{Cl}^-}$ and $c^{\text{gel}}_{\text{Na}^+}$ are the internal concentration concentrations of monovalent anions and cations in the internal solution, c_{s} is the salinity of the external solution, V_{gel} v_{gel} is the gel molar volume (inverse density of gel segments) and α is the ionization degree (in the case of our study $\alpha = 1$). The "$\pm$" sign in the formula accounts for the change between sign change for the cases of gel made of polyanion or polycation gels.

The lower salinity solution As shown in [13,15–17], the solution of lower salinity can be extracted from the gel by means of compression and/or other stimulus providing stimuli, provided that the charge of in the gel remains constant. In the case of gel made of weak weak polyelectrolyte (pH-sensitive) polyelectrolytegel, the compression discharges the gel , and therefore the neutralizing counterions leave out the gel, diminishing the desalination effect [19].

One can argue that the sole Donnan effect is insufficient to achieve a high salt rejection [7] and the salinity of the water squeezed from hydrogel under a very high hydraulic pressure (up to 100 bar [16]) turns out to be not much different from the initial. Indeed, the use of high hydraulic pressure diminishes all the advantages of this method over RO,

and the reversibility of hydrogel swelling after strong compression remains questionable. Nevertheless, in ~~the current~~ this study, we model the compression of the gel limiting ourselves to low compression rates, less than 5 bar, and studied how the compression of the gel affects the surrounding salinity. We ~~modelled also~~ modeled the desalination process, as a cascade of ~~following one by each other~~ step-by-step gel swellings and compressions, driving the salinity of the supernate down to ~~drinkable water.~~ potable water.

2. Model and methods

3. ~~Theory behind the simulation~~

2.1. Open and closed sytems

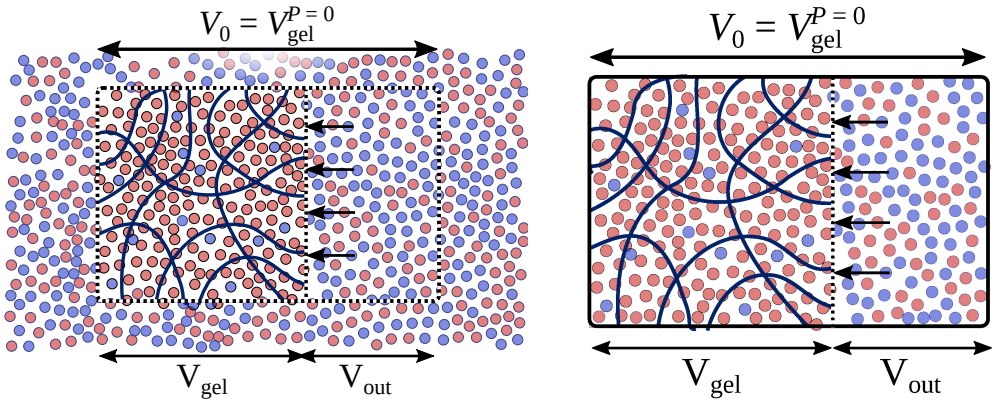

(a) Open system **(b)** Closed system

Figure 1. Diamond-like network in the simulation box. Color code represents the individual ion types (red: Na^+, blue: Cl^-, yellow: Ca^{2+}) and the hydrogel (~~gray~~grey: neutral segment (AH), cyan: charged segment (A^-)). .

2.2. ~~Model~~

We propose the desalination process as a cascade of gel compressions and decompressions lowering the supernatant salinity. In this process, the gel is supposed to be compressed/decompres in an *open system* and in a *closed system*. The compression in *open system* assumes that the gel is in thermodynamic equilibrium with a huge (effectively **infinite**) reservoir of an aqueous solution, whereas the *closed system* implies that the gel is in equilibrium with a **finite** reservoir of an aqueous solution.

By thermodynamic equilibrium, we assume that the gel freely exchanges ions with the reservoir. Thus, the *open system* implies the grand canonical ensemble of mobile ions, in which the change of free energy due to ion exchange is accounted for by their chemical potential. The *closed system* is the Gibbs ensemble of ions moving between two volumes of the gel phase and the supernatant.

Due to huge size of the reservoir, the compression of the gel in *open system* does not affect the reservoir salinity, $c_s = c_{Na^+} = c_{Cl^-} = \text{Const}$, whereas the number of ions entrapped in the volume V_0 changes (Figure 1a). On the contrary, the compression of the gel in the *closed system* changes the salinity in the reservoir, but the total number of Na^+ and Cl^- ions in the gel and in the reservoir, *i.* e. in the volume V_0 (Figure 1b), remains constant.

The mechanical movement and the exchange of ions occur simulataneously in reality, however, we simulate them alternating each other in stop-run mode. To sample mechanical properties of the gel and reservoir we use MD simulation, whereas to sample the ions distribution between the gel and a reservoir we use MC simulation. The details of this hybrid MCMD computational technique can be found in our previous studies of polyelectrolytes in open system [18,20,21].

2.2. Molecular Dynamics

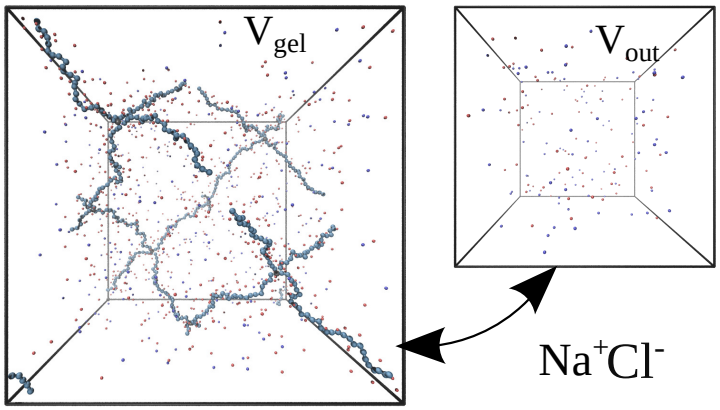

Figure 2. Diamond-like network in the simulation box. Color code represents the individual ion types (red: Na^+, blue: Cl^-, yellow: Ca^{2+}) and the hydrogel (gray: neutral segment (AH), cyan: charged segment (A^-)). .

We model the gel as a network of 16 linear polymer chains, each ~~by~~ consisting of 30 monomer units. ~~The~~ These polymer chains are connected to a diamond-like ~~polymer network throught~~ network by 8 crosslinking units~~, and put into a simulation box with periodic boundaries~~. This means, there are $N_{gel} = 16 \cdot 30 + 8 = 488$ gel monomers in the simulation box (see Figure 2). ~~Each~~ The network is put in simulation cubic box of the volume V_{gel} with periodic boundary conditions, which virtually emulaates an infinite polymer network.

Each monomer unit of the network carries a negative ~~electric charge, which is equal to the charge of electron. Except the particles of the network~~elementary electric charge. Except for the gel monomers, the monovalent co- and counter-ions ions, Cl^- and Na^+, are present in the simulation box. The total electric charge of all the particles in the box is zero, therefore the amount of Na^+ ions ~~is bigger than that~~ exceeds the amount of Cl^- by ~~the number of hydrogel units, $N_{gel} = 16 \cdot 30 + 8 = 488$~~ N_{gel}.

~~We simulate the compression of the gel in two ensembles.~~

1. ~~The first is so called *open system*, when the simulation box with gel freely exchanges ions with a big amount of aqueous solution of certain constant salinity, c_s.~~
2. ~~The second is *closed system*, when the gel is in equilibrium with a finite volume of aqueous solution.~~

~~The compression of the gel in the *open* system does not affect the surrounding salinity, thus the density of ions outside the gel remains constant $c_s = c_{Na^+} = c_{Cl^-} = \text{Const}$ (Figure 1a) . On the contrary, what remains constant in the *closed* system, is~~ Each pair of the particles interact via the truncated Lennard-Jones interaction potential, which imposes strong repulsion between all particles at short distances:

$$V_{LJ}(r) = \begin{cases} 4\varepsilon\left(\left(\frac{\sigma}{r}\right)^{12} - \left(\frac{\sigma}{r}\right)^{6}\right) & \text{if } r < r_{cut} \\ 0 & \text{elsewhere} \end{cases}, \quad (2)$$

where r is the ~~total number of Na^+~~ interparticle distance, $\sigma = 0.35$nm is a chosen characteristic size of the particles, $\varepsilon = k_B T$ is the depth of the potential and r_{cut} is the cut-off distance beyond which the potential is set zero.

The bonds connecting the gel to a network are modeled using finite extension nonlinear elastic potential (FENE)

$$V_{\mathrm{FENE}}(r) = -\frac{1}{2}K\Delta r_{\max}^2 \ln\left[1 - \left(\frac{r - r_0}{\Delta r_{\max}}\right)^2\right], \tag{3}$$

where r is the distance between the bonded segments, K is the magnitude of their interaction, $\Delta r_{\max}$ is the maximal stretching length of the bond and r_0 is the equilibrium bond length. For our simulations we chose $K = 10k_{\mathrm{B}}T/\sigma^2$, $\Delta r_{\max} = 2\sigma$ and ~~Cl^- ions, that are contained in the gel and in the external volume, *i.* e. in the volume V_0 (Figure 1b)~~$r_0 = 1.0\sigma$ [22].

All the charged paticles interact via Coulomb electrostatic potential:

$$N_i V_{\mathrm{EL}} = N_i^{\mathrm{gel}} + c_{\mathrm{s}} \cdot (V_0 - V_{\mathrm{gel}}) l_{\mathrm{B}} k_{\mathrm{B}} T \frac{q_1 q_2}{r}, \tag{4}$$

where ~~$i \in \{\mathrm{Na}^+, \mathrm{Cl}^-\}$, N_i is~~ l_{B} is Bjerrum length; $l_{\mathrm{B}} = 2\sigma = 0.7\mathrm{nm}$ which corresponds to the Bjerrum length in water at temperature $T = 300\mathrm{K}$, k_{B} — Botlzman constant. In that sense, the ~~amount of the corresponding ions in gel, V_{gel}~~solvent (water) accounted for in the model implicitly via setting up dielectric permittivity $\epsilon = 80$.

We used Langevin thermostat, *i.* e. the two additional terms to force in equation of motion were added

$$\mathbf{f}_i = -\gamma \mathbf{v}_i(t) + \sqrt{2\gamma k_{\mathrm{B}} T}\boldsymbol{\eta}_i(t), \tag{5}$$

where the first term correspond to constant friction with γ being a friction coefficient, and the second one corresponds to random thermal force with $\boldsymbol{\eta}_i$ being a normally distributed random vector; $\mathbf{v}_i$ — ~~volume of the gel, V_0 — the volume in which the gel is compressed. As V_0 we choose the volume of the gel in the free swelling equilibrium state~~velocity of i-th particle (see for details [23]).

~~Diamond-like network in the simulation box. Color code represents the individual ion types (red: Na^+, blue: Cl^-, yellow: Ca^{2+}) and the hydrogel (gray: neutral segment (AH), cyan: charged segment (A^-)). .~~

2.3. ~~*Open* *~~Monte Carlo sampling in open *system.*~~

~~We simulate the open system using the grand reaction method [18,21]. This method is a hybrid of molecular dynamics (MD) and Monte Carlo (MC). The whole simulation represents a chain of subsimulations of MD and MC followed one by each other. For MD simulation we used a standard Langevin dynamics [23] which models the mechanical movement of all the system particles . Whereas MC simulates the thermodynamic equilibrium with reservoir, which exchanges ions with~~ Monte Carlo scheme for sampling the exchange of ions in *open system* is based on the formula for free energy of grand canonical ensemble, Ω

$$\Omega_{\mathrm{open}} = E - TS + \sum_i \mu_i N_i \tag{6}$$

where E is internal energy, T — temperature, S — entropy, N_i is the number of ions of type $i \in \{\mathrm{Na}^+, \mathrm{Cl}^-\}$, μ_i — corresponding chemical potential.

The entropy S is given by the Boltzmann formula [24]

$$S = k_{\mathrm{B}} \sum_i \ln \frac{V_{\mathrm{gel}}^{N_i}}{N_i!} \tag{7}$$

which accounts for two contributions:

1. the combinatorial entropy $S_c = -k_B \sum_i \ln N_i!$ which reflects the freedom of choice among the particles
2. the mixing entropy $S_m = k_B \sum_i N_i \ln V_{gel}$ which reflects the freedom to place the chosen particle randomly within the simulation box. ~~The insertion (and deletion)~~

V_{gel} is the unitless volume, *i.* e. the volume measured in units of σ^3. Thus the change of free energy associated with an exchange of ion pairs is ~~considered as a reaction of creation (or annihilation) of an ion pair~~

$$\varnothing \overset{K}{\leftrightarrows} Na^+ + Cl^-$$

$$\Delta\Omega_{open} = k_B T \ln \prod_i \left(V_{gel}^{\xi} \frac{N_i!}{(N_i+\xi)!} \right) + \xi \sum_i \mu_i + \Delta E \tag{8}$$

~~with a reaction constant defined by the chemical potential of ions, $K = \exp(\mu_{Na^+} + \mu_{Cl^-})$.~~ where ξ is an algebraic number of inserted (or removed) ion pairs; in general ξ can be any number, but in the case when $\xi = \pm 1$, which corresponds to addition or removal of only one ion pair, the Equation 8 gets simplified

$$\Delta\Omega_{open} = k_B T \ln V_{gel}^{2\xi} \prod_i (N_i + \theta(\xi))^{-\xi} + \xi \sum_i \mu_i + \Delta E \tag{9}$$

where θ is the Heaviside function, $\theta(\xi) = 1$, if $\xi = +1$, $\theta(\xi) = 0$, if $\xi = -1$.

2.4. ~~*Closed system.*~~

~~The similar scheme we use to simulate the gel in closed system . The procedure represents a chain of subsequent MD and MC simulation, but now the molecular dynamics is running in two simulation boxes simultaneously. The first box of the volume V_{gel} contains the gel with ions,~~ The procedure of the Monte Carlo Sampling is the following [25]

1. propose the new configuration of the system by insertion (or deletion) of an ion pair, $\xi = \pm 1$
2. accept the new configuration if

$$\mathcal{R}^{\xi} < e^{\Delta\Omega_{open}/k_B T} = V_{gel}^{2\xi} \prod_i (N_i + \theta(\xi))^{-\xi} e^{(\Delta E + \xi\mu)/k_B T} \tag{10}$$

   where $\mathcal{R}$ is uniformly distributed random number in range between 0 and ~~the second box, V_{out} — contains only ions~~1.
3. then collect the number of ions, N_{Na^+} and N_{Cl^-} to the samples array.

2.4. *Monte Carlo sampling in closed system*

In the *closed system* the gel exchanges particles with explicit finite reservoir box. The total ~~volume of~~ number of ion species in both boxes is ~~kept constant, $V_0 = V_{gel} + V_{out}$, so the compression of the gel implies the decreasing V_{gel} and increasing V_{out}. These two boxes are represented in Figure 2.~~

2.5. ~~*Algorithm.*~~

~~The~~ fixed, whereas the density of ions in extrernal reservoir is defined by thermodynamic equilibrium between the two ~~volumes implies the exchange of ion pairs between them, which is done by means of MC procedure~~ subvolumes (see Figure 1b. The Monte Carlo sampling of the distribution of ions between the subvolumes performed in a way similar to described in ~~[26]. The simulation~~ [26,27].

The free energy of the Gibbs ensemble is a sum of the gel's free energy and that of the external volume.

$$\Omega_{\text{closed}} = E_{\text{gel}} - TS_{\text{gel}} + E_{\text{out}} - TS_{\text{out}} \tag{11}$$

using similar reasoning as for *open system* one can derive the change of free energy associated with ion pair exchange

$$\Delta\Omega_{\text{closed}} = 2k_BT \ln\left(\frac{V_{\text{gel}}}{V_{\text{out}}}\right) \xi \prod_i \left(\frac{N_i^{\text{gel}} + \theta(\xi)}{N_i^{\text{out}} + \theta(-\xi)}\right)^{-\xi} + \Delta E_{\text{gel}} + \Delta E_{\text{out}} \tag{12}$$

where ξ defines the direction of the trial move, so that $\xi = -1$ when an ion pair moved from gel to outside volume and $\xi = +1$ otherwise, ΔE_{gel} and ΔE_{out} are corresponding changes of the potential energy of the gel and the outside volumes.

Then the procedure of sampling is the same as that for *open sysytem*: (1) propose the move of an ion pair, (2) accept a new state if $\mathcal{R}^{\xi} < \exp(\Delta\Omega_{\text{closed}}/k_BT)$, (3) repeat the procedure until the desired number of samples is reached.

2.5. Algorithm

As mentioned above, the whole simulation run consists of MD and MC subsimulations of mechanical movement of the particles and ion exchange. The algorithm is following:

1. ~~Simulate molecular dynamics in both boxes;~~ Initiate the systems to simulate: the gel of the volume V_{gel} and the external solution of the volume V_{out};
2. Equilibrate the system running interspersing the MD and MC stages
3. Run the MD subsimulation and collect the observables~~, for example, values of pressure P, to an array~~: pressure in both volumes, P_{gel}, P_{out}, and distancies between the nodes of the gel network. The last one needed to estimate the autocorrelation of MD simulation;
4. ~~Perform Monte-Carlo~~ Run MC procedure simulating ion ~~pair exchange ; collect the arrays of observables samples:~~ exchange and collect the number of ions in both boxes, $N_{\text{Cl}^-}^{\text{gel}}$ and $N_{\text{Cl}^-}^{\text{out}}$;
5. Repeat the ~~procedure~~ MD and MC subsimulations until the desired length of sample arrays is reached.

3. ~~Results and discussion~~

Using the data obtained from simulations we calculate c_s — the density of ions in the outside volume; v_{gel} — molar volume of the gel, *i.* e. the volume of the gel per one mol of gel segments, $v_{\text{gel}} = V_{\text{gel}}/N_{\text{gel}}$, n_{Cl^-} — the total amount of the ions in both volumes divided by the total volume of both boxes, $n_{\text{Cl}^-} = N_{\text{Cl}^-}/V_0$ and Π — *partial pressure* of the gel, *i.* e. the pressure that needs to be applied to the gel via a solvent permeable filter to compress the gel to a specific molar volume. We obtain the gel partial pressure as a difference between the presure in gel and in the outer volume $\Pi = P_{\text{gel}} - P_{\text{out}}$.

The volume V_0 was chosen to be close to the gel free swelling equilibrium, that is to the state where $\Pi = 0$. In order to obtain the value V_0 we perform the set of open system simulations for various V_{gel}. That value of V_{gel}, at which Π is closest to zero we choose as V_0. Then, as soon as V_0 is defined, we perform the compression of the gel in *closed system* varying values of $V_{\text{gel}} < V_0$ and $V_{\text{out}} = V_0 - V_{\text{gel}}$.

3. Results and discussion

3.1. Compression in open system~~.~~

~~First~~So, at the beginning, we run a set of simulations modeling the gel compression in *open system*, *i. e.* in equilibrium with a big bath of certain salinity, c_s. The simulations ~~are~~ were run for a set of different ~~simulation box volumes~~gel volumes, V_{gel}. Each simulation

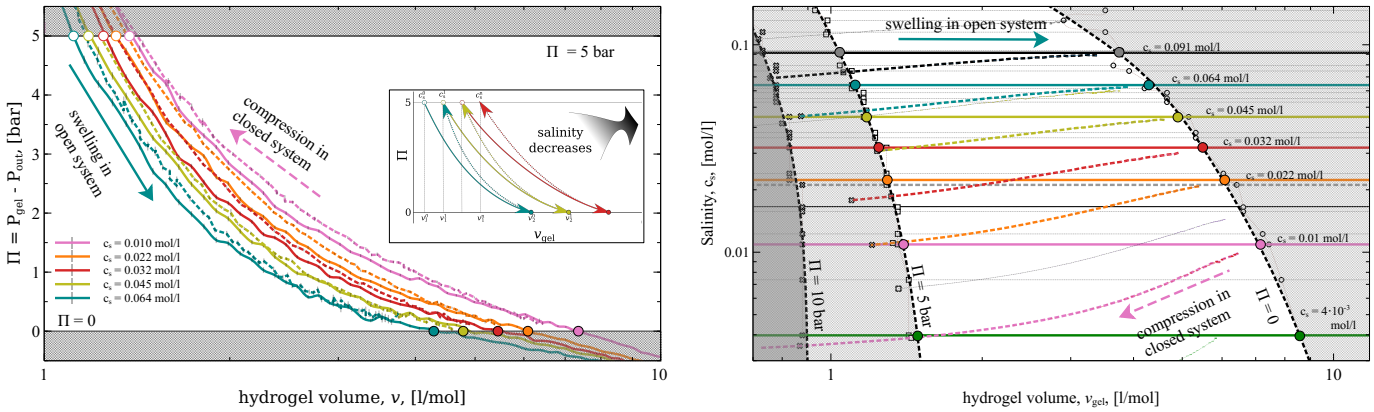

(a) The gel partial pressure vs gel molar volume

(b) Supernate salinity vs gel molar volume

Figure 3. The compression of the gel in ~~open system~~ the *open system* (solid lines) and in ~~closed system~~ the *closed system* (dotted lines). Each solid curve corresponds to different salinity of the reservoir c_s (see legend). ~~Shadowed area~~ The shadowed areas limit the states with applied pressure below zero and above 5 bar.

~~returns the averaged pressure, P~~returned the averaged values of pressures, P_{gel}, and the number of Cl^- ions, ~~which are~~ present in the simulation box, ~~n_{Cl^-}.~~

~~In order to get the partial pressure of the gel, we substitute from P the osmotic pressure of ions in the reservoir: $\Pi = P - P_{out}$. P_{out}, in turn, we calculate by running a separate simulation of a reservoir, containing ionic gas in equilibrium with the bath of the same salinity c_s. The gel partial pressure, Π, is the pressure that needs to be applied to the gel via a solvent permeable filter to compress the gel to a specific molar volume, V_{gel}. By gel molar volume V_{gel} we assume the volume of the gel calculated per on mol of gel monomer units~~ $N^{gel}_{Cl^-}$.

The dependencies of Π on V_{gel} ~~are present in Figure 3a~~ for *open system* for a set of ~~different salinities . These dependencies (the case of *open system*) are represented~~ various salinities are presented in Figure 3a by solid lines. For example, the blue solid line illustrates the compression (or swelling) of the gel in equilibrium with a reservoir of salinity, $c_s = 0.063$ mol/l. The points where the pressure equals zero, $\Pi = 0$, (indicated by filled circles) are the gel *free swelling equilibrium* states. These states are characterized by the corresponding molar volume of the gel, V^0_{gel} and the amount of ions in gel $\{N^0_{Na^+}, N^0_{Cl^-}\}$ (Index "0" stands for zero bar applied pressure). The *free swelling equilibrium* states' positions shift towards smaller volumes with increase of salinity. In general, the increase of salinity ~~shift~~ shifts all the $\Pi(V)$ curves towards smaller volumes. This effect is well known and is typical for all branched *strong* polyelectrolytes. It is caused by the decrease of ions osmotic pressure and by a screening of electrostatic interactions [21,28]. [1] (The salinity dependence of the size of *weak* polyelectrolyte gel is in general non-monotonic. We discuss this case in [19].)

3.2. Compression in closed system

~~*The free swelling equilibrium states are characterized by the corresponding molar volume of the gel,*~~

The simulations in *closed systems* start from the V^0_{gel} and ~~the amount of ions in gel~~ $\{N^0_{Na^+}, N^0_{Cl^-}\}$ ~~(Index "0" stands for zero bar applied pressure). We use these states as the starting ones for the gel compression in~~ values obtained from the corresponding ~~*closed*~~ *open system*~~. Thus, we simulate the compression of the gel~~ simulations. The simulation of gel compression in a closed volume, V_0, ~~which is equal to V^0_{gel}, and contains~~ starts at the

[1] ~~The salinity dependence of the size of *weak* polyelectrolyte gel is in general non-monotonic. We discuss this case in [19].~~

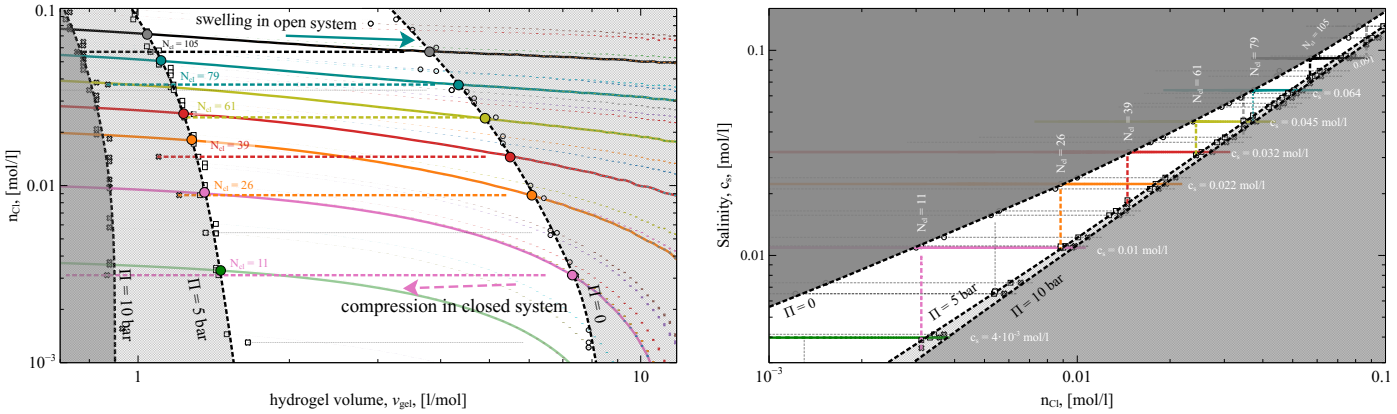

(a) Pressure vs gel molar volume

(b) Salinity vs gel molar volume

Figure 4. The compression of the gel in *open system* (solid lines) and in *closed system* (dotted lines). Shadowed area limit the states with applied pressure below zero and above 5 bar. The values N_{Cl^-} are the virtual numbers of present Cl^- ions in *closed system* simulation boxes.

point $V_0 = V^0_{gel}$ and ion content $N^0_{Cl^-}$ ~~of~~ for Cl^- ions~~and the~~. The Na^+ ions ~~in the amount neutralizing~~ amount is neutralize the system, $N^0_{Na^+} = N^0_{Cl^-} + N_{gel}$.

We prepare two systems~~, one — simulating the gel of~~: one for simulation of the gel at the volume V_{gel}, and ~~another — simulating~~ the other one for simulation of the supernatant solution ~~of~~ at the volume $V_{out} = V_0 - V_{gel}$. ~~Also,~~ Note that the ions of the amount $N^0_{Cl^-}$ and $N^0_{Na^+}$ are shared ~~between~~ by the two volumes.

The processes of the gel compression in *closed system* are depicted in Figure 3a as dotted lines. In this plot, for example, the blue dotted line ~~, for example,~~ illustrates the compression of the gel equilibrated with the solution of salinity $c_s = 0.063$ mol/l ~~, in a volumewhich~~ at volume, at which the gel has at zero pressure. ~~Since, in this case, the volumes of the gel~~ The volume values V_{gel} and ~~of the supernate~~ V_{out} are comparable ~~, the compression of the gel decreases the salinity of~~ in the *closed system* case. Therefore, the gel compression causes decrease of the salinity in the supernate, c_s. This dependence is illustrated in Figure 3b, where the same swelling/compression processes are displayed in different coordinates: *i. e.* salinity of supernate versus the gel molar volume, $c_s(V_{gel})$. In these coordinates, all the open system compressions show up as horizontal lines, which reflects the constant salinity, whereas the compressions in closed system demonstrate the change of c_s from $c^0_s = 0.063$ at zero pressure Π to $c^5_s = 0.045$ mol/l at $P^{gel} = 5$ bar (index "5" stands for 5 bar).

Although the salinity during compression in *open system* remains constant, the ~~number~~ amount of ions in ~~a compression volume,~~ the compressed subsystem (*i. e.* in the volume where the gel is compressed (or swells)), changes. ~~In the Figure 4a we depicted the~~ Here, the compression volume V_0 is the volume of the *free swelling equilibrium* state of the gel, $V_0 = V^0_{gel}$. Figure 4a shows number of Cl^- ions in the volume V_0 ~~, calculated~~ per unit volume, $n_{Cl^-} = N_{Cl^-}/V_0$, as a function of the gel molar volume. The depicted ~~value~~ values can be considered as the average density of Cl^- ions ~~averaged out over~~ in the compression volume V_0.

~~As expected in the case of closed system compression these~~ The n_{Cl^-}-V_{gel} dependencies look like horizontal lines ~~, whereas in an open system, the amount of ions in compressionvolume increases with compression~~in the case of *closed system* compression, whereas n_{Cl^-} increases with V_{gel} during the compression in the *open system* case. This implies, that the compression of the gel in the ~~open system~~ *open system* pulls out the ions from the bath to the compression volume, V_0. And vice versa, the swelling of the gel pushes ions out to the bath.

Finally, ~~in Figure 4b~~ the same processes are depicted in Figure 4b in coordinates n_{Cl^-} — c_s. In these coordinates, both ways of the compression, in *open* and in *closed* ~~system~~systems, appear as straight vertical and horizontal lines correspondingly.

In our study, we modeled the compression of the gel in equilibrium with reservoirs of 40 different salinities, ranging from 0.001 to 0.5 mol/l. ~~Every open system compression~~ The *open system* compressions resulted in a defined free swelling equilibrium ~~state~~states, which we used as the initial ~~ones for the compression in closed systems~~conditions for the respective compressions in *closed systems*. All the corresponding dependencies are depicted in Figures 3 and 4 as thin grey dashed lines (some of them are highlighted and colored). The states corresponding to $P^{gel} = 0$, 5 and 10 bar pressure are marked by open circles, squares, and crosses respectively. The non-shadowed areas in the Figures highlight the states in which the gel partial pressure ranges between the experimentally relevant values, 0 and 5 bar.

3.3. Desalination scheme~~.~~

~~As we have seen,~~ It follows that the compression of the gel in ~~a closed system~~ the *closed system* affects the salinity, whereas the compression in ~~an open system~~ the *open system* affects the amount of ions in ~~a volume where the gel is compressed in~~the gel subsystem. Here we show how to employ these phenomena for water desalination. The highlighted colored lines on plots of Figures 3 and 4 form a sequence ~~of the following one by each other~~ gel swellings and compressions~~of the hydrogel~~, following one by one, correspondingly in *open* and *closed* systems. This sequence forms the water desalination process. Starting from swelling the gel in the *open system* at high salinity ($c_s = 0.091$ mol/l, solid black line), the gel ~~gets compressed in~~ is compressed in the *closed system* until the pressure reaches 5 bar (dashed black line). Then the same gel swells in a reservoir of a bit lower salinity in the *open system* (*i. e.* $c_s = 0.064$ mol/l, light blue line). After the swelling, the gel is compressed again ~~by the pressure of~~ with the pressure 5 bar in *closed system* (dashed light blue line). Then the gel ~~is put swelling~~ swells in a reservoir of even smaller salinity ($c_s = 0.045$ mol/l, solid yellow line)~~. And~~, and so on. ~~The~~ This chain of alternating ~~swelling and compression steps~~ swellings and compressions ends up when salinity ~~gets~~ is equal to $c_s = 4 \cdot 10^{-3}$ mol/l after ~~compression in closed system~~ the compression in the *closed system* (dashed magenta line).

The plots ~~of~~ in Figures 3 and 4 depict the whole process in all ~~the possible coordinates In all the plots~~possible coordinate representations. In all plots, the lines corresponding to sequential swellings and compressions during the whole desalination process resemble a 'pathway'. In particular, the ~~whole process looks like a staircase, especially in the~~ desalination process depicted in Figure 4b ~~, where open system~~ resembles a staircase, where the *open system* processes are horizontal lines and ~~closed system are vertical ones, a 'staircase' has rectangular steps~~ the *closed system* processes are vertical lines.

3.4. The efficiency of desalination~~.~~

The theoretical minimum specific energy for seawater desalination ($c_s \simeq 0.6$ mol/l as for pure NaCl) is ~ 3.9 kJ/l (1.1 kWh/m^3) for 50% recovery [29]. This value is calculated as follows

$$W_{id} = 2RT\left(\frac{c_f}{R_w}\ln\frac{c_b}{c_f} - c_p \ln\frac{c_b}{c_p}\right) \tag{13}$$

where R is a universal gas constant, c_f is the salinity of feed water, c_p ~~—~~is the salinity of product water and c_b ~~—~~is the salinity of the brine, which necessarily appears in any desalination process. R_w is a recovery ratio, *i. e.* the ratio between the volume of produced water and the volume of the feed water. 50% recovery ratio means that one part of feed water divides into two equal volume solutions of the product water and of the brine. Of course, a significant amount of additional energy is required to operate the system[30]. It has been reported that the specific energy consumption (SEC) of the reverse osmosis (RO) process is 2.5 – 4.0 kWh/m3 (~~9~~9.0 – 14.4 kJ/l), which is significantly higher than its

minimum specific energy. The SEC of a real-scale RO plant is even higher, approximately 3.5 – 4.5 kWh/m^3 (12.6 - 16.2 kJ/~~L~~l), including pre-treatment and post-treatment processes [31].

~~In order to~~ To compare the efficiency of the desalination process presented in ~~3 and 4~~ Figure 3 and Figure 4 with provided values, we collect the corresponding data to ~~the~~ Table 1. The presented desalination process is a cascade of six swellings in an open system, at six different (constant) salinities c_s, each followed by six compressions in a closed system, at six different (constant) n_{Cl^-}. Each swelling and compression process is presented as a row of Table 1, which is colored by matching the lines in the Figures. The first column of the table contains values c_s^0 and c_s^5, which stand for the supernate salinity at 0 and 5 bar compression; in an open system, supernate salinity does not change, so c_s^0 and c_s^5 are presented by a single number. The second column contains values of n^0 and n^5, which stand for the number of Cl^- ions in compression volume V_0, at 0 and 5 bar pressure (divided by V_0). The number of ~~ion~~ ions does not change in closed system compression, thus n^0 and n^5 are the same in the corresponding rows. The third column shows the change of the gel volume in the corresponding process, Δv. The fourth column ~~contain~~ contains the work needed for the compression in the corresponding process ~~, calculated~~ per volume of extracted solution. This value is ~~an integral~~ obtained as numerical integration of corresponding $\Pi(V_{gel})$ dependence [32]

$$W = \frac{\int_{v^0}^{v^5} \Pi dV_{gel}}{\Delta v} \tag{14}$$

~~Here, in the table, we present~~ In this column, we presented the absolute values of the work, whereas one should keep in mind that ~~the compression implies~~compression implies, that the work is done by external force and ~~the swelling implies~~swelling implies, that the work is done by gel.

To give a clue of comparison with ideal desalination process efficiency, ~~in~~ the fifth column ~~we provided~~ provides the values of ideal specific energy consumption, W^{id}, which are calculated ~~by means of Equation 13as follows. We consider, for example, the solution of concentration~~ employing Equation 13, for concentrations of feed, product and brine solutions, c_s^f, c_s^p, c_s^b, as indicated by curly brackets. For example, having c_s^f = 44.91~~mmol/l as a feedsolution, and the solutionsof~~ , c_s^p = 31.93 ~~mmol/l~~ and c_s^b = 63.93 mmol/l~~correspondingly as produced product and brine solutions.~~ , (5th, 7th and 3rd rows of the table) one can imagine the following desalination process

1. ~~first~~First, the gel ~~, equilibrated with~~ equilibrated with the feed solution, is ~~getting compressed in a closed system. The volume of the gel changes~~ compressed in the *closed system*. The gel volume decreases by Δv^p = 3.69 ~~l~~ liters and the salinity of supernate decreases from c_s^f to c_s^p. The volume of ~~product solution equals~~ the product solution is Δv^p
2. ~~Then the~~ The squeezed gel is put back into the feed solution and is ~~getting~~ equilibrated there under pressure, so it does not swell.
3. After ~~equilibration~~ the equilibration, the gel swells in the ~~gel is let to swell in a closed system such that~~ *closed system*, so the salinity of the external solution increases ~~reaching the value of~~ to the value c_s^b.
4. Finally, the gel is taken out and ~~squeezed by 5 bar in an open system~~ compressed by pressure 5bar in the *open system* in equilibrium with the ~~bath of the brine~~ brine bath. The change of the gel volume in this process is Δv^b = 3.26 l/mol, which equals the volume of the produced brine.

Thus the recovery ratio $R_w = \Delta v^p/(\Delta v^p + \Delta v^b) \simeq 0.53$ and the theoretical minimum specific energy of ~~desalination~~ the desalination process with corresponding c_s^f, c_s^p and c_s^b is W^{id} = 38.2 J/l (Equation 13).

Table 1. The estimates of the efficiency of the desalination process. All the units are calculated per one mol of gel segments. Values in brackets are the estimates corresponding to crossection of 'red' and 'orange' lines on the plots of Figures 3 and 4

c_s^0, mM	c_s^5, mM	$n^0_{Cl^-}$, mM	$n^5_{Cl^-}$, mM	ΔV_{gel}, l	$\lvert W \rvert$, J/l	W^{id}, J/l
91.47		57.08 ± 0.122	$\longrightarrow$ 71.75 ± 0.024	2.74	95.4 ± 1.9	
89.41 ± 0.23	$\longrightarrow$ 73.63 ± 0.03	56.90		2.72	109.1 ± 1.7	
63.93		37.28 ± 0.08	$\longrightarrow$ 50.579 ± 0.013	3.26	100.9 ± 1.7	
62.05 ± 0.15	$\longrightarrow$ 48.21 ± 0.02	37.17		3.18	107.4 ± 1.4	
44.91		23.75 ± 0.06	$\longrightarrow$ 35.911 ± 0.010	3.82	106.7 ± 1.5	
43.46 ± 0.12	$\longrightarrow$ 30.795 ± 0.008	24.27		3.91	106.4 ± 1.1	
31.93		14.66 ± 0.04	$\longrightarrow$ 25.297 ± 0.006	4.20	107.9 ± 1.4	
30.03 ± 0.08	$\longrightarrow$ 18.585 ± 0.004 (22.32)	14.55		4.17 (3.22)	115.6 ± 0.9 (57.3)	
22.30		8.84 ± 0.03	$\longrightarrow$ 17.945 ± 0.004 (14.56)	4.75 (3.76)	108.1 ± 1.3 (68.3)	
20.74 ± 0.06	$\longrightarrow$ 11.082 ± 0.002	8.83		4.71	110.8 ± 0.8	
10.90		3.00 ± 0.01	$\longrightarrow$ 9.011 ± 0.002	6.08	106.9 ± 1.1	
9.83 ± 0.05	$\longrightarrow$ 3.862 ± 0.001	3.12		5.78	119.4 ± 1.0	

$W^{id} = 52.9$, $W^{sim} = 202.8 \pm 3.2$, $R_w = 0.54$

$W^{id} = 43.8\ (41.0)$, $W^{sim} = 222.3 \pm 2.5$, $R_w = 0.52\ (0.46)$

$W^{id} = 69.7$, $W^{sim} = 227.5 \pm 2.3$, $R_w = 0.55$

$W^{id} = 38.2$, $W^{sim} = 207.3 \pm 2.2$, $R_w = 0.53$

$W^{id} = 66.6\ (22.0)$, $W^{sim} = 218.7 \pm 2.2$, $R_w = 0.53\ (0.49)$

~~Such estimations~~ The estimated W^{id} values are provided in the fifth column of the table, for five triplets of ~~values~~ c_s^f, c_s^p, ~~and~~ c_s^b ~~.~~ values. In the same column we provide W_{sim} ~~is the energy calculated by —~~ the specific energy consumptions calculated by a numerical integration of $\Pi(V_{gel})$ dependencies ~~— sum of corresponding comressions in closed and open systems, W_{id} — the estimate based on the equation Equation 13 and~~ . The provided values W_{sim} are the sum of energies needed for corresponding compression processes, *i.* e. in *closed* and *open* systems. The values R_w ~~— is~~ , which are also provided in 5th colum are the corresponding recovery ~~ratio. Note~~ ratios.

The ratio between W_{sim} and W_{id} ranges from 3.26 to 5.43, which is comparable to that of RO. Note, that calculating the W_{sim} we accounted for only the work done on the gel during the compression, whereas the work done by the gel itself during swelling was not taken into account. The ~~ratio between W_{sim} and W_{id} ranges from 3.26 to 5.43, which is comparable to that of RO~~process, which accounts for the energy recovery was described in our previous studies [19,33]

3.5. *Study limitations*

Like other simulation based studies, our research has a limited validity, primarily resulting from the simplifications applied in the used model. For example, our coarse-grained model cannot differentiate polystyrene sulphonate gel from other strong polyacidic gels. However, these limitations are also the advantage of our model because the results of our study can be applied to similar systems, including polybasic gels with all the charges reversed.

3.6. *Implications and future perspectives*

We are aware that the concept introduced in this simulation study need to be experimentally verified. Therefore, in the future, we want to focus on experimental aspects of desalination based on polyacidic gel compression.

4. Conclusions

We have modeled the compression of the polyelectrolyte gel in thermodynamic equilibrium with the ~~reservoir of the limited amountof water~~supernatant aqueous solution of a limited amount. We have shown that ~~in the case of gel made of strong polyelectrolyte, the compression always decreases the surrounding~~ the compression of the gel decreases the supernatant salinity. We ~~have modeled~~ employed this phenomenon for modeling the process of water desalination~~by combining~~ . The desalination was done as a sequential combination of two processes: (1) ~~the~~ swelling of the gel in *open system*, exchanging ions with a big reservoir at constant salinity~~.~~ ; (2) ~~the~~ compression of the gel in *closed system*, when the gel ~~affects the salinityin the surrounding solution~~exchanges ions with a small reservoir affecting its salinity. We estimated the energy ~~needed to produce~~ consumption needed for producing one liter of ~~water~~ potable water from brine and have shown that the proposed gel compression method may compete with ~~the modern technologies used in modern industry~~modern desalination technologies.

Author Contributions: Conceptualization, O.R. ; methodology, M.L.; software, M.L.; validation, M.L., L.N. and O.R.; formal analysis, L.N.; data curation, M.L.; writing—original draft preparation, O.R.; writing—review and editing, L.N.

Funding: "This research was funded by Czech Science Foundation grant number 19-17847Y" and Government of Russian Federation grant number 14.W03.31.0022.

Acknowledgments: This research was supported by the Czech Science Foundation (grant 19-17847Y) Government of Russian Federation, grant number 14.W03.31.0022.

Conflicts of Interest: The authors declare no conflict of interest.

References

1. Guesmi, A.; Cherif, M.M.; Baaloudj, O.; Kenfoud, H.; Badawi, A.K.; Elfalleh, W.; Hamadi, N.B.; Khezami, L.; Assadi, A.A. Disinfection of corona and myriad viruses in water by non-thermal plasma: a review. *Environ Sci Pollut Res* **2022**, *29*, 55321–55335. doi:10.1007/s11356-022-21160-7.
2. Baaloudj, O.; Badawi, A.K.; Kenfoud, H.; Benrighi, Y.; Hassan, R.; Nasrallah, N.; Assadi, A.A. Techno-economic studies for a pilot-scale Bi12TiO20 based photocatalytic system for pharmaceutical wastewater treatment: From laboratory studies to commercial-scale applications. *Journal of Water Process Engineering* **2022**, *48*, 102847. doi:10.1016/j.jwpe.2022.102847.
3. Shahzad, W.; Badawi, A.K.; Rehan, Z.A.; Khan, A.M.; Khan, R.A.; Shah, F.; Ali, S.; Ismail, B. Enhanced visible light photocatalytic performance of Sr0.3(Ba,Mn)0.7ZrO3 perovskites anchored on graphene oxide. *Ceramics International* **2022**, *48*, 24979–24988. doi:10.1016/j.ceramint.2022.05.151.
4. Miller, J. Review of Water Resources and Desalination Technologies. Technical report, 2003. doi:10.2172/809106.
5. Curto, D.; Franzitta, V.; Guercio, A. A Review of the Water Desalination Technologies. *Applied Sciences* **2021**, *11*, 670. doi:10.3390/app11020670.
6. Akther, N.; Sodiq, A.; Giwa, A.; Daer, S.; Arafat, H.A.; Hasan, S.W. Recent advancements in forward osmosis desalination: A review. *Chemical Engineering Journal* **2015**, *281*, 502–522. doi:10.1016/j.cej.2015.05.080.
7. Cai, Y.; Hu, X.M. A critical review on draw solutes development for forward osmosis. *Desalination* **2016**, *391*, 16–29. doi:10.1016/j.desal.2016.03.021.
8. Wack, H.; Ulbricht, M. Effect of synthesis composition on the swelling pressure of polymeric hydrogels. *Polymer* **2009**, *50*, 2075–2080. doi:10.1016/j.polymer.2009.02.041.
9. Tanaka, T.; Nishio, I.; Sun, S.T.; Ueno-Nishio, S. Collapse of Gels in an Electric Field. *Science* **1982**, *218*, 467–469. doi:10.1126/science.218.4571.467.
10. Serizawa, T.; Wakita, K.; Akashi, M. Rapid Deswelling of Porous Poly(N-isopropylacrylamide) Hydrogels Prepared by Incorporation of Silica Particles. *Macromolecules* **2001**, *35*, 10–12. doi:10.1021/ma011362+.
11. Lietor-Santos, J.J.; Sierra-Martin, B.; Vavrin, R.; Hu, Z.; Gasser, U.; Fernandez-Nieves, A. Deswelling Microgel Particles Using Hydrostatic Pressure. *Macromolecules* **2009**, *42*, 6225–6230. doi:10.1021/ma9010654.
12. Qiu, Y.; Park, K. Environment-sensitive hydrogels for drug delivery. *Advanced Drug Delivery Reviews* **2001**, *53*, 321–339. doi:10.1016/s0169-409x(01)00203-4.
13. Li, D.; Zhang, X.; Yao, J.; Simon, G.P.; Wang, H. Stimuli-responsive polymer hydrogels as a new class of draw agent for forward osmosis desalination. *Chem. Commun.* **2011**, *47*, 1710. doi:10.1039/c0cc04701e.
14. Wang, H.; Wei, J.; Simon, G.P. Response to Osmotic Pressure versus Swelling Pressure: Comment on "Bifunctional Polymer Hydrogel Layers As Forward Osmosis Draw Agents for Continuous Production of Fresh Water Using Solar Energy". *Environmental Science and Technology* **2014**, *48*, 4214–4215. doi:10.1021/es5011016.
15. Arens, L.; Albrecht, J.B.; Höpfner, J.; Schlag, K.; Habicht, A.; Seiffert, S.; Wilhelm, M. Energy Consumption for the Desalination of Salt Water Using Polyelectrolyte Hydrogels as the Separation Agent. *Macromol. Chem. Phys.* **2017**, *218*, 1700237. doi:10.1002/macp.201700237.
16. Fengler, C.; Arens, L.; Horn, H.; Wilhelm, M. Desalination of Seawater Using Cationic Poly(acrylamide) Hydrogels and Mechanical Forces for Separation. *Macromol. Mater. Eng.* **2020**, *305*, 2000383. doi:10.1002/mame.202000383.
17. Ali, W.; Gebert, B.; Hennecke, T.; Graf, K.; Ulbricht, M.; Gutmann, J.S. Design of Thermally Responsive Polymeric Hydrogels for Brackish Water Desalination: Effect of Architecture on Swelling, Deswelling, and Salt Rejection. *ACS Appl. Mater. Interfaces Applied Materials and Interfaces* **2015**, *7*, 15696–15706. doi:10.1021/acsami.5b03878.
18. Rud, O.V.; Landsgesell, J.; Holm, C.; Košovan, P. Modeling of weak polyelectrolyte hydrogels under compression – Implications for water desalination. *Desalination* **2021**, *506*, 114995. doi:10.1016/j.desal.2021.114995.
19. Rud, O.; Borisov, O.; Košovan, P. Thermodynamic model for a reversible desalination cycle using weak polyelectrolyte hydrogels. *Desalination* **2018**, *442*, 32–43. doi:10.1016/j.desal.2018.05.002.
20. Rud, O.V.; Kazakov, A.D.; Nova, L.; Uhlik, F. Polyelectrolyte Hydrogels as Draw Agents for Desalination of Solutions with Multivalent Ions. *Macromolecules* **2022**, *55*. doi:10.1021/acs.macromol.1c02266.
21. Landsgesell, J.; Hebbeker, P.; Rud, O.; Lunkad, R.; Košovan, P.; Holm, C. Grand-Reaction Method for Simulations of Ionization Equilibria Coupled to Ion Partitioning. *Macromolecules* **2020**, *53*, 3007–3020. doi:10.1021/acs.macromol.0c00260.
22. Jin, S.; Collins, L.R. Dynamics of dissolved polymer chains in isotropic turbulence. *New Journal of Physics* **2007**, *9*, 360. doi:10.1088/1367-2630/9/10/360.
23. Grest, G.S.; Kremer, K. Molecular dynamics simulation for polymers in the presence of a heat bath. *Physical Review A* **1986**, *33*, 3628–3631. doi:10.1103/PhysRevA.33.3628.
24. Nagle, J.F. Regarding the Entropy of Distinguishable Particles. *Journal of Statistical Physics* **2004**, *117*, 1047–1062. doi:10.1007/s10955-004-5715-5.
25. Frenkel, D.; Smit, B. *Understanding Molecular Simulation*; Academic Press, San Diego, 2002.
26. Panagiotopoulos, A.; Quirke, N.; Stapleton, M.; Tildesley, D. Phase equilibria by simulation in the Gibbs ensemble. *Molecular Physics* **1988**, *63*, 527–545. doi:10.1080/00268978800100361.
27. Erdos, M.; Galteland, O.; Bedeaux, D.; Kjelstrup, S.; Moultos, O.A.; Vlugt, T.J.H. Gibbs Ensemble Monte Carlo Simulation of Fluids in Confinement: Relation between the Differential and Integral Pressures. *Nanomaterials* **2020**, *10*, 293. doi:10.3390/nano10020293.

28. Zhulina, E.; Klein Wolterink, J.; Borisov, O. Screening Effects in a Polyelectrolyte Brush: Self-Consistent-Field Theory. *Macromolecules 23 (2000). - ISSN 0024-9297* **2000**, *33*. doi:10.1021/ma990187i.
29. Wang, L.; Violet, C.; DuChanois, R.M.; Elimelech, M. Derivation of the Theoretical Minimum Energy of Separation of Desalination Processes. *Journal of Chemical Education* **2020**, *97*, 4361–4369. doi:10.1021/acs.jchemed.0c01194.
30. Kim, J.; Park, K.; Yang, D.R.; Hong, S. A comprehensive review of energy consumption of seawater reverse osmosis desalination plants. *Applied Energy* **2019**, *254*, 113652. doi:10.1016/j.apenergy.2019.113652.
31. Kim, J.; Hong, S. A novel single-pass reverse osmosis configuration for high-purity water production and low energy consumption in seawater desalination. *Desalination* **2018**, *429*, 142–154. doi:10.1016/j.desal.2017.12.026.
32. Atkins, P.; de Paula, J. *Physical Chemistry, Ninth Edition*; Oxford University Press, New York, 2010.
33. Prokacheva, V.M.; Rud, O.V.; Uhlík, F.; Borisov, O.V. Phase transition in hydrophobic weak polyelectrolyte gel utilized for water desalination. *Desalination* **2021**, *511*, 115092. doi:10.1016/j.desal.2021.115092.